



## Study of additive correction multigrid application

**Diego Fernando Moro**

difmoro@ufpr.br; difmoro@gmail.com

Department of Mechanical Engineering, Positivo University

R. Prof. Pedro Viriato Parigot de Souza, 5300 - Cidade Industrial, Curitiba-PR, Brazil.

**Carlos Henrique Marchi**

chmcfd@gmail.com

Department of Mechanical Engineering, Federal University of Paraná

Av. Coronel Francisco H. dos Santos, 100 - Jardim das Américas, Curitiba-PR, Brazil.

**Abstract.** *There are a lot of problems in engineering, some of them can be modeled through mathematical model equations without greater error addition. An analytical solution for these models equations are generally unknown, so one uses a numerical method to solve them. In this work, the Finite Volume Method (FVM) is employed to solve the following model equations: Burgers 1D, Poisson 2D and Poisson 3D. The linear system of equations resulted from FVM is solved using the Additive Correction Multigrid (ACM) strategy with Gauss-Seidel solver, the singlegrid is also tested and a comparison between them is shown. The coefficient of complexity, i.e., the rate which the CPU time increases in relation to the size of the grid doesn't reach exactly the unity, which is the theoretical complexity coefficient of Multigrid strategy, but a possible explanation to this fact is shown.*

**Keywords:** *Multigrid, Finite Volume Method, Additive Correction Multigrid*

## 1 INTRODUCTION

Nowadays engineering problems are solved using a mixed of theory and empiricism. In any case, solving problems using the theory, through mathematical models, usually the analytical solution is unknown. This is the reason why numerical methods are used to obtain its solution and commonly these mathematical models are composed of systems of partial differential equations and/or integrals.

There are lot of numerical methods for solving differential equations, the simplest is the Finite Difference Method (Fortuna, 2000 & Incropera; DeWitt, 2003) which is based in a direct approximation of the derivatives of differential equation throughout the nodes of the grid. In the other hand the Finite Volume Method (Maliska, 2010) is based in the discretization of the domain in control volumes, which the conservation equations are integrated, the terms resulted from this integration are approximated, be differential or integral terms.

Once that the approximation has been applied, algebraic equations are generated and must be solved somehow. Solvers, are used for this purpose, but the convergency rate, i.e., the speed which these methods get closer to the numeric solution is sometimes very slow.

### 1.1 Multigrid

It is possible to ally these solvers with a methodology named multigrid (Briggs; Henson & McCormick, 2000), which presents some properties which increase the convergency rate and reduce the computational time to obtain the numerical solution. There are two groups within multigrid methodologies: geometrical and algebraic. The first one presents in general the smaller computational time and is easier to understand and apply but is not as generic as the second one which presents a greater CPU time.

The Additive Correction Multigrid (ACM) (Keller, 2007) can be considered an algebraic methodology but is simpler to understand and apply than most algebraic multigrid methods (Briggs; Henson & McCormick, 2000). The reason is that this methodology is based only in the coefficient matrix of the linear system generated from the discretization, thus can be applied independently from the numerical method used.

As an example, consider the volume 5\* of the coarse grid in Fig. 1, this coarse volume is composed of volumes 15, 16, 21 and 22 of the fine grid. The coefficients and source term of the volume 5\* are calculated as an restriction of the volumes composed shown in the Eq. (1).

$$\begin{aligned}a_s(5^*) &= a_s(15) + a_s(16) \\a_w(5^*) &= a_w(15) + a_w(21) \\a_P(5^*) &= a_P(15) + a_P(16) + a_P(21) + a_P(22) - \\&[a_e(15) + a_n(15) + a_w(16) + a_n(16) + a_s(21) + a_e(21) + a_s(22) + a_w(22)] \\a_e(5^*) &= a_e(16) + a_e(22) \\a_n(5^*) &= a_n(21) + a_n(22) \\b_P(5^*) &= r(15) + r(16) + r(21) + r(22)\end{aligned}\tag{1}$$

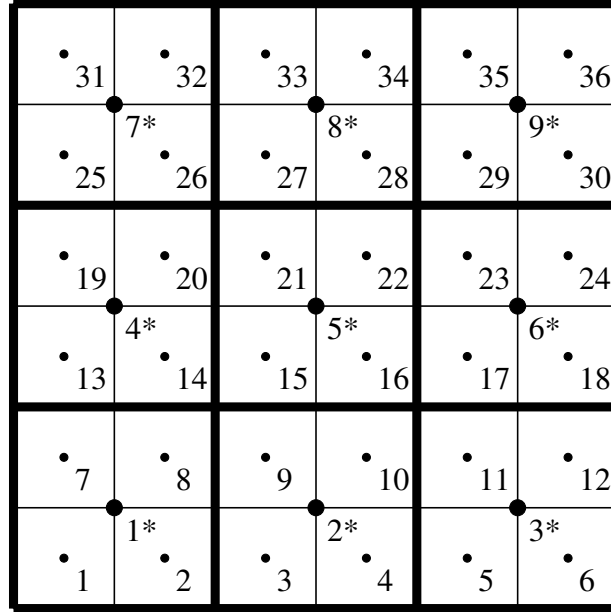


Figure 1: Example of applied 2D ACM

where  $r$  is the residual of linear system in the analysed volume ( $\{r\}=[A] \{x\}-\{b\}$ ).

This coefficients and source terms are obtained to solve the correction (Eq. (2)) for the entire coarse volume, i.e. in the previous example, the correction must be used in volumes 15, 16, 21 and 22 through the Eq. (3).

$$[A] \{c\} = \{b\} \quad (2)$$

where  $c$  is the correction.

$$\phi = \phi^* + c \quad (3)$$

where  $\phi^*$  is the previous value and  $\phi$  is the corrected value.

## 1.2 Goals

The goal of this work is to apply the additive correction multigrid methodology in three model problems: Burgers 1D, Poisson 2D e Poisson 3D. The numerical implementation will be analysed as well as the computational time and the complexity coefficient of the implemented multigrid methodology.

## 1.3 Finite volume method

The Finite Volume Method (Maliska, 2010) is based on the integration of differential equation over control volumes, which the domain is divided. An illustrative generic onedimensional uniform grid is shown in Fig. 2, where grid size  $h$  is given by  $h = \frac{L}{N}$  where  $N$  is the total

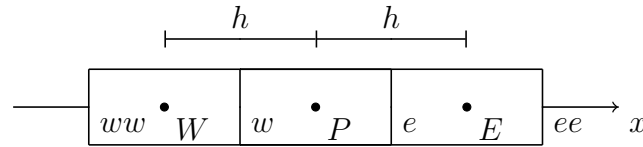


Figure 2: Generic 1D grid for the discretization of the domain

number of volumes used in that direction. In all the model problems solved, the grids were uniform in each direction.

where,  $W$ ,  $P$  and  $E$  are the nodes of the volumes and  $ww$ ,  $w$ ,  $e$  and  $ee$  are the faces of these volumes.

## 2 Mathematical and numerical models

In this section the mathematical and numerical models of selected problems are shown.

The secondary variables in each model problem, there is the calculation of the average. This average will be calculated using the numeric integration of rectangle rule (Chapra; Canale, 2015).

### 2.1 Burgers 1D

The Burgers 1D problem can model several physical problems which include but are not limited to: a onedimensional laminar flow of a fluid of constant properties. The differential equation of this model problem is given by Eq. (4).

$$Re \frac{du^2}{dx} = \frac{d^2u}{dx^2} + S(x) \quad (4)$$

where  $Re$  is the Reynolds number of the flow, defined by  $Re = \frac{\rho UL}{\mu}$ , where  $\rho$  is the density of the fluid and  $\mu$  is the dynamic viscosity.

The source term is given by:  $S(x) = Re^2 e^{xRe} \frac{2e^{xRe} - e^{Re} - 1}{(e^{Re} - 1)^2}$  was obtained through the fabricated solutions method, and allow an analytic solution proposed by Eq. (5).

$$u(x) = \frac{e^{xRe} - 1}{e^{Re} - 1} \quad (5)$$

The boundary conditions are given by Eq. (5) in the limits of the used unitary domain  $0 \leq x \leq 1$  and are  $u(1) = 0$  and  $u(N) = 1$ , in this work:  $Re = 100$ .

The secondary variables analysed are: (1) velocity in the domain center, which is obtained by a linear interpolation between neighbour volumes and (2) velocity average, which is given by Eq. (6).

$$\bar{u} = \frac{1}{L_x} \int_0^1 u(x) dx = \frac{e^{Re} - Re - 1}{Re(e^{Re} - 1)} \quad (6)$$

Applying the integration over the control volume, second order approximation for the differential terms, linearization of the quadratic terms and rectangle rule for the integration terms, one can obtain a system of algebraic equations which are a threedagonal, which the general equation is given by Eq. (7) and the coefficients and source terms are given by Eq. (8).

$$a_P u_P = a_e u_E + a_w u_W + b_P \quad (7)$$

$$\begin{aligned} P &= 1, \dots, N \\ a_P &= 8 + Reh(u_E^* - u_W^*) \\ a_e &= 4 - Reh(u_P^* + u_E^*) \\ a_w &= 4 + Reh(u_W^* + u_P^*) \\ b_P &= 4h^2 S_P \end{aligned} \quad (8)$$

where  $u_W^*$ ,  $u_P^*$  and  $u_E^*$  are the velocities known in the previous iteration.

The boundary conditions application is made using the fictitious volumes method. Therefore, external volumes are created in all the external faces, which will have the coefficients and source terms obtained by an interpolation between the real and fictitious volumes, this interpolation is exactly equal to the boundary condition in that face.

The solution behaviour of this problem for the following Reynolds number: 1, 5, 25 and 125 is shown in Fig. 3.

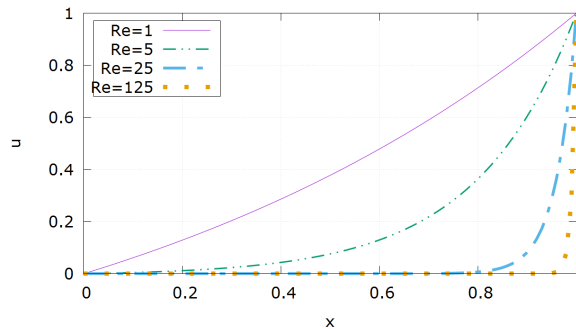


**Figure 3: Burgers 1D, solution behaviour for Re = 1, 5, 25 and 125. Adapted from Moro & Marchi (2016)**

## 2.2 Poisson 2D and 3D

The Poisson 2D problem can model several physical problems which include but are not limited to: heat conduction with internal heating source, laminar incompressible flow in a plane of a pipe in a completely developed flow or still in the stream function-vorticity formulation, two Poisson 2D equations-like are solved to obtain a laminar incompressible twodimensional flow. The differential equation of this model problem is given by Eq. (9).

$$\frac{\partial^2 T}{\partial x^2} + \frac{\partial^2 T}{\partial y^2} + S(x, y) = 0 \quad (9)$$

The source term is given by:  $S(x, y) = 2 \pi^2 \sin(\pi x) \sin(\pi y)$ , was obtained through the fabricated solutions method, and allow an analytic solution proposed by Eq. (10).

$$T(x, y) = \sin(\pi x) \sin(\pi y) \quad (10)$$

The boundary conditions are null in all the faces of the unitary plate between  $0 \leq x, y \leq 1$ .

The secondary variables analysed are: (1) temperature in the domain center, which is obtained by a linear interpolation between neighbour volumes and (2) temperature average, which is given by Eq. (11).

$$\bar{T} = \frac{1}{L_y} \frac{1}{L_x} \int_0^1 \int_0^1 T(x, y) dx dy = \frac{4}{\pi^2} \quad (11)$$

Applying the integration over the control volume, second order approximation for the differential terms and rectangle rule for the integration terms, one can obtain a system of algebraic equations which are a fivediagonal, which the general equation is given by Eq. (12) and the coefficients and source terms are given by Eq. (13).

$$a_P T_P = a_s T_S + a_w T_W + a_e T_E + a_n T_N + b_P \quad (12)$$

$$\begin{aligned} P &= 1, \dots, N \\ a_s &= a_w = a_e = a_n = 1 \\ a_P &= 4 \\ b_P &= h^2 S_P \end{aligned} \quad (13)$$

The boundary conditions application folow the same methodology used in the previous model problem.

The solution behaviour of this problem is shown in Fig. 4 obtained using the VisIt (Childs et al., 2012) application, this software was developed by the Department of Energy (DOE) Advanced Simulation and Computing Initiative (ASCI) of US.

The Poisson 3D problem can model several physical problems which include but are not limited to: heat conduction with internal heating source. The differential equation of this problem is given by Eq. (14).

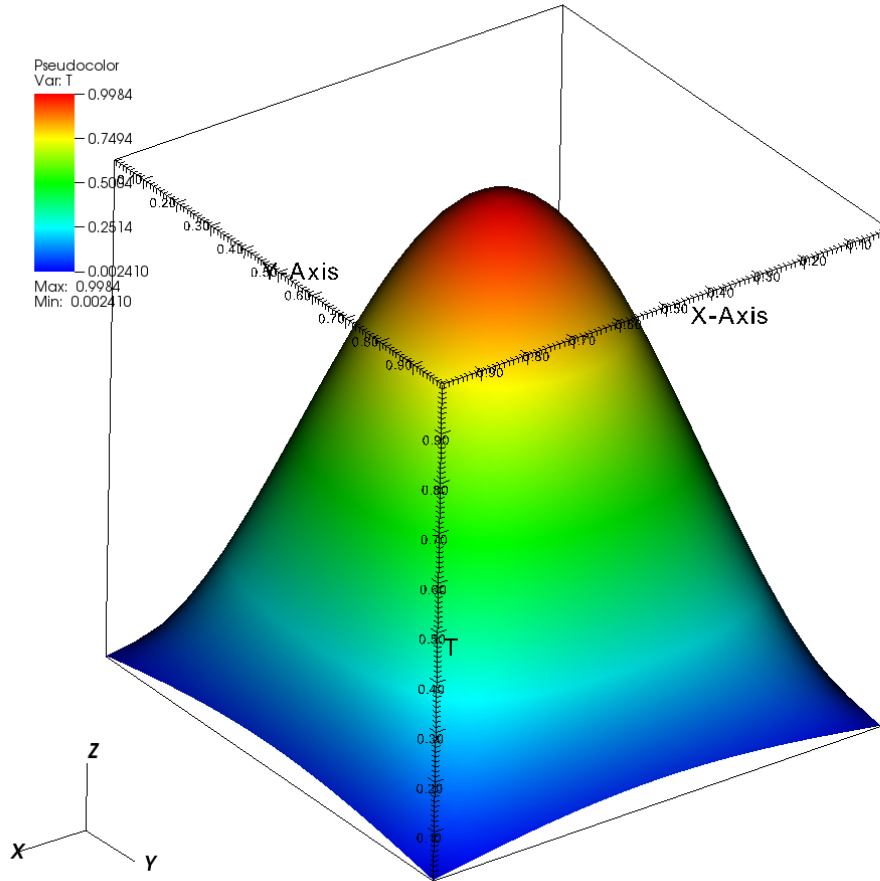


Figure 4: Poisson 2D, solution behaviour

$$\frac{\partial^2 T}{\partial x^2} + \frac{\partial^2 T}{\partial y^2} + \frac{\partial^2 T}{\partial z^2} = -S(x, y, z) \quad (14)$$

The source term is given by:  $S(x, y, z) = 3 \pi^2 \sin(\pi x) \sin(\pi y) \sin(\pi z)$ , was obtained through the fabricated solutions method, and allow an analytic solution proposed by Eq. (15).

$$T(x, y, z) = \sin(\pi x) \sin(\pi y) \sin(\pi z) \quad (15)$$

The boundary conditions are null in all the faces of the unitary cube between  $0 \leq x, y, z \leq 1$ .

The secondary variables analysed are: (1) temperature in the domain center, which is obtained by a linear interpolation between neighbour volumes and (2) temperature average, which is given by Eq. (16).

$$\bar{T} = \frac{1}{L_z} \frac{1}{L_y} \frac{1}{L_x} \int_0^1 \int_0^1 \int_0^1 T(x, y, z) dx dy dz = \frac{8}{\pi^3} \quad (16)$$

Applying the integration over the control volume, second order approximation for the differential terms and rectangle rule for the integration terms, one can obtain a system of algebraic equations which are a sevendagonal, which the general equation is given by Eq. (17) and the coefficients and source terms are given by Eq. (18).

$$a_P T_P = a_d T_D + a_s T_S + a_w T_W + a_e T_E + a_n T_N + a_u T_U + b_P \quad (17)$$

$$P = 1, \dots, N$$

$$a_d = a_s = a_w = a_e = a_n = a_u = 1 \quad (18)$$

$$a_P = 6$$

$$b_P = h^2 S_P$$

The solution behaviour of this problem is shown in Fig. 5, again obtained using the VisIt application, for three planes of the unitary cube.

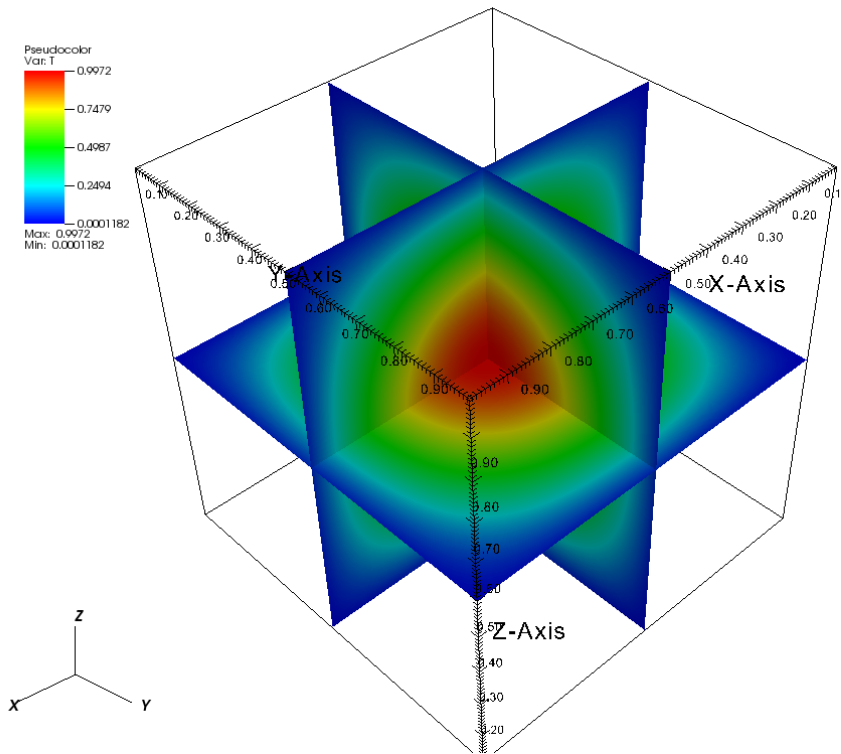


Figure 5: Poisson 3D, solution behaviour in three planes of the unitary cube

### 2.3 Stopping criteria, initial guess and more information

The used stopping criteria was a tolerance of  $10^{-10}$  for the average  $L_1$  norm of linear system residual (Eq. (19)), if  $|\overline{L_1}|$  was smaller than the tolerance applied, the iterative system was stopped.

$$|L_1| = \frac{\sum_{i=1}^N |Ax - b|}{N} \quad (19)$$

where  $A$  is the matrix of the linear system,  $x$  is the unknown vector and  $b$  is the source term vector.

The initial guess used in each model problem was the analytical solution. The PC used was a Asus B85M-E/BR, Intel Core i7-4790 3.6 GHZ with 8 GB of RAM memory, using Windows 7 64 Bit. The code language used was Fortran 95, the compiler version: Intel Fortran 15.0.115.2010.

In this work, in 1D ACM application, two volumes of the fine grid become one volume in the coarse grid, and in 2D ACM four volumes become one and in 3D ACM eight volumes become one. In Fig. 1 is shown an example of 2D ACM.

The number of solver sweeps in the V cycle were: one iteration for the fine grid, two for the restriction and for prolongation.

## 2.4 Effective and apparent orders

In the verification procedure of a numerical code, one should analyse if the numerical solution approximate from analytical solution, i.e. if the finer the grid the lesser discretization error, and if the numerical accuracy is close to the teoretical one, i.e. if the second order scheme applied in this work really gives this order of accuracy.

The effective and apparent orders are used to obtain the true orders of numerical error, if both are close to two, this gives confidence that the code is solving the problem accordingly.

If one consider a three grid solution,  $\phi_1$ ,  $\phi_2$  and  $\phi_3$  (where the subscript 1 is the coarser and 3 is the finest) and an analytical solution  $\Phi$ , with a constant refinement ratio of  $r$ . The effective and apparent order of the finer grid are given by Eq. (20) and (21) for effective and apparent order respectively.

$$p_E = \frac{\log\left(\frac{\Phi - \phi_2}{\Phi - \phi_3}\right)}{\log(r)} \quad (20)$$

$$p_U = \frac{\log\left(\frac{\phi_2 - \phi_1}{\phi_3 - \phi_2}\right)}{\log(r)} \quad (21)$$

## 3 Results

The results obtained for each model problem are shown in this section.

### 3.1 Burgers 1D

For this model problem the following real volumes were used in the discretization: 2, 4, 8, 16, 32, 64, 128, 256, 512, 1 024, 2 048, 4 096, 8 192, 16 384, 32 768, 65 536, 131 072, 262 144, 524 288, 1 048 576 and 2 097 152.

The Fig. 6 show the discretization error, i.e., the difference between analytical solution and numerical solution, for both secondary variables analysed in relation with the number of volumes used.

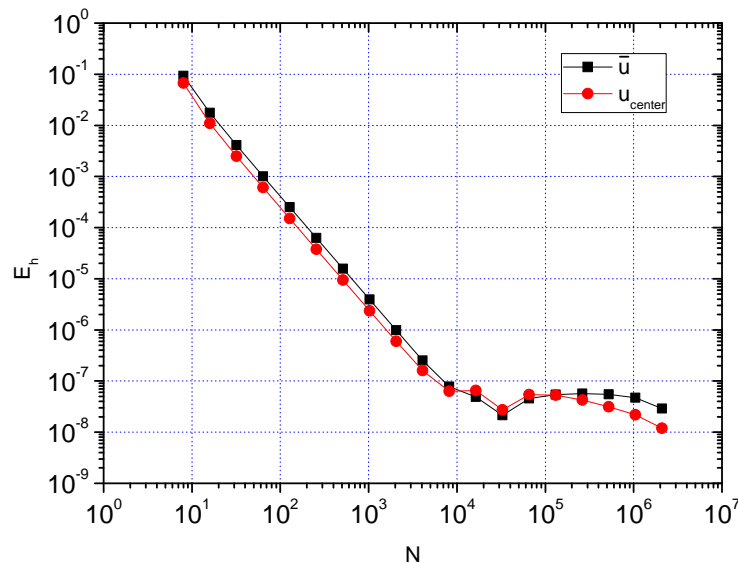


Figure 6: Burgers 1D, discretization error of the secondary variables

The Fig. 7 show the effective and apparent orders, i.e., the rate which the discretization error decreases in relation with the increase of the numbers of volumes used for both secondary variables analysed.

Finally, the Fig. 8 show the computational time and a exponential fit to show the complexity coefficient of the implemented additive correction multigrid method.

### 3.2 Poisson 2D and 3D

For these model problems the following real volumes were used in the discretization:  $2^2$ ,  $4^2$ ,  $8^2$ ,  $16^2$ ,  $32^2$ ,  $64^2$ ,  $128^2$ ,  $256^2$ ,  $512^2$ ,  $1\,024^2$ ,  $2\,048^2$  and  $4\,096^2$  in Poisson 2D;  $2^3$ ,  $4^3$ ,  $8^3$ ,  $16^3$ ,  $32^3$ ,  $64^3$ ,  $128^3$  and  $256^3$  in Poisson 3D problem.

The Figs. 9 and 10 show the discretization error, i.e., the difference between analytical solution and numerical solution, for both secondary variables analysed in relation with the number of volumes used.

The Figs. 11 and 12 show the effective and apparent orders, i.e., the rate which the discretization error decreases in relation with the increase of the numbers of volumes used for both secondary variables analysed.

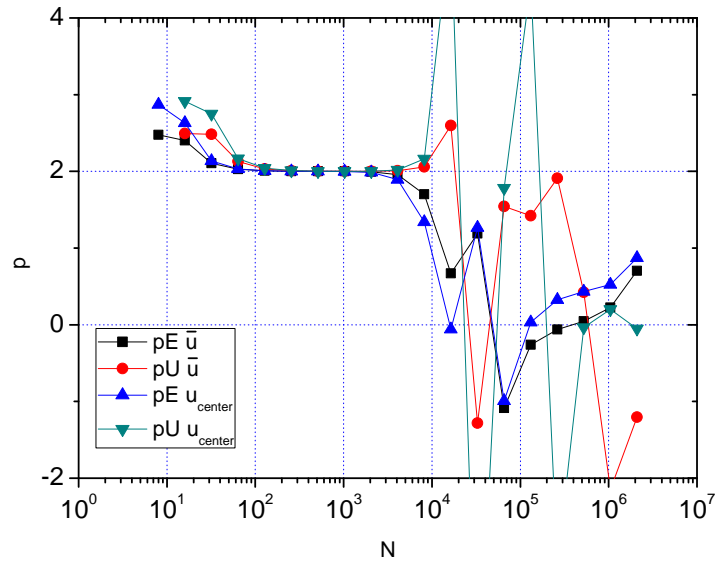


Figure 7: Burgers 1D, effective and apparent orders of the secondary variables

Finally, the Figs. 13 and 14 show the computational time and a exponential fit to show the complexity coefficient of the implemented additive correction multigrid method.

## 4 Discussion and conclusion

The goal of this work was to apply the additive correction multigrid methodology in three model problems: Burgers 1D, Poisson 2D and Poisson 3D.

The finite volume method was used and a set of algebraic equations were obtained, which was the starting point for the Additive Correction Multigrid strategy, the solver used was Gauss-Seidel in each linear system.

Through Figs. 6, 9 and 10 for  $E_h$ , and Figs. 7, 11 and 12 for the true orders of numerical error of numerical scheme applied, one can analyse that when the discretization error is greater than iteration errors, i.e. until intermediate number of volumes ( $\approx 10^4$  in 1D,  $\approx 2 \cdot 10^5$  in 2D and not reached in 3D), the true orders are getting closer and closer to the second order approximation scheme applied. But if refined even further, as the stopping criteria is fixed in a tolerance of  $10^{-10}$  of the average  $L_1$  norm of the residuals, the iteration errors became more significantly.

Through Figs. 8, 13 and 14 is possible to analyse that the complexity coefficient obtained through a exponential fit of the computational time versus problem size (number of volumes) for ACM is not close to the teoretical unity as obtained through Keller (2007) or Briggs; Henson & McCormick (2000), but 1.56 for 1D, 1.44 for 2D and 1.11 for 3D. The singlegrid is also compared, the bigger number of volumes, the higher speedup obtained from multigrid.

A possible explanation for these results is the following: it is possible to analyse that in the geometric Poisson 1D multigrid correction scheme using Finite Differences Method (Brigs; Henson & McCormick, 2000), the residual on a restriction of the coarse volume (correction

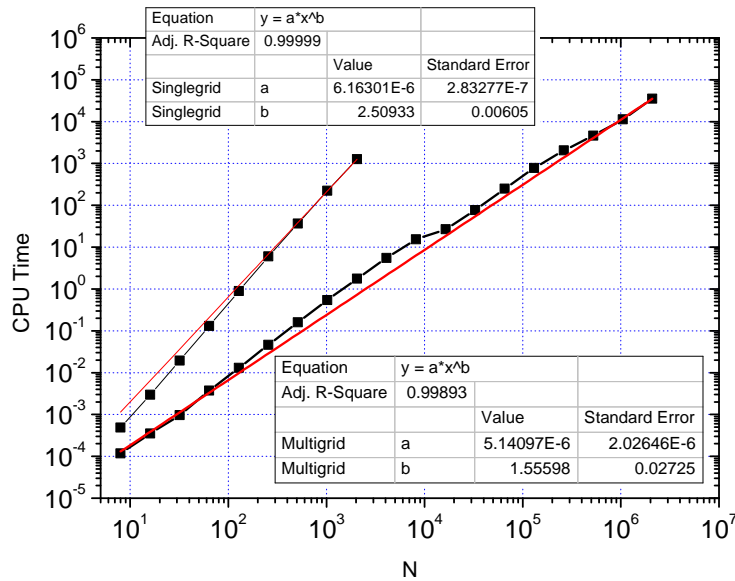


Figure 8: Burgers 1D, computational time with complexity coefficient

linear system) will be  $r^2$  greater than in the fine volume (where  $r$  is the refinement ratio, 2 in each direction for this work). This means that a four times greater residual is expected, but the restriction operator in Additive Correction Multigrid is basically the sum of residuals, so the residual in the coarse grid is just two times greater.

Better studies about the behaviour of this strategy should be made, specially because of the easy implementation and generic application.

## ACKNOWLEDGEMENTS

The authors thank the UNIESPAÇO Program of the AEB (Brazilian Space Agency), CNPq (Conselho Nacional de Desenvolvimento Científico e Tecnológico, Brazil), and CAPES (Coordenação de Aperfeiçoamento de Pessoal de Nível Superior, Brazil) for their financial support. The first author was scholarship of CAPES and nowadays is a Positivo University professor. The second author is scholarship of CNPq.

## REFERENCES

- Briggs, W. L., Henson, V. E. & McCormick, S. F., 2000. A multigrid tutorial, SIAM, 2ed.
- Chapra, S. C. & Canale, R. P., 2015. Numerical Methods for Engineers, New York: McGraw-Hill Education.
- Fortuna, A. O., 2000. Técnicas computacionais para a dinâmica dos fluidos. Edusp, So Paulo.
- Incropera, F. P. & DeWitt, D. P., 2003. Fundamentos de Transferência de Calor e de Massa. LTC, Rio de Janeiro, 5 ed.

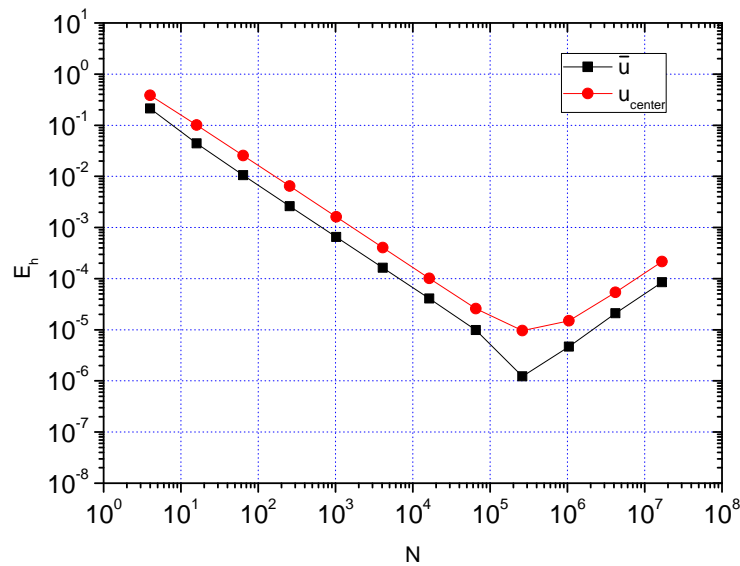


Figure 9: Poisson 2D, discretization error of the secondary variables

Keller, S. C, 2007. O método multigrid de correções aditivas para a solução numérica acoplada das equações de Navier-Stokes com malhas não-estruturadas. PhD thesis, Universidade Federal de Santa Catarina, Florianópolis.

Maliska, C. R, 2010. Transferência de calor e mecânica dos fluidos computacional. LTC, Rio de Janeiro, 2 ed.

Marchi, C. H, 2001. Verificação de soluções numéricas unidimensionais em dinâmica dos fluidos. PhD thesis, Universidade Federal de Santa Catarina, Florianópolis.

Moro, D. F. & Marchi, C. H., 2016. Formulação de volumes finitos para as faces. Simpósio de Métodos Numéricos em Engenharia, Universidade Federal do Paraná, Curitiba.

Childs, H., Brugger, E., Whitlock, B., Meredith, J., Ahern, S., Pugmire, D., Biagas, K., Miller, M., Harrison, C., Weber, G. H., Krishnan, H., Fogal, T., Sanderson, A., Garth, C., Bethel, E. W., Camp, D., Rübel, O., Durant, M., Favre, J. M. & Navrátil, P., 2012. VisIt: An End-User Tool For Visualizing and Analyzing Very Large Data, High Performance Visualization—Enabling Extreme-Scale Scientific Insight pp. 357-372.

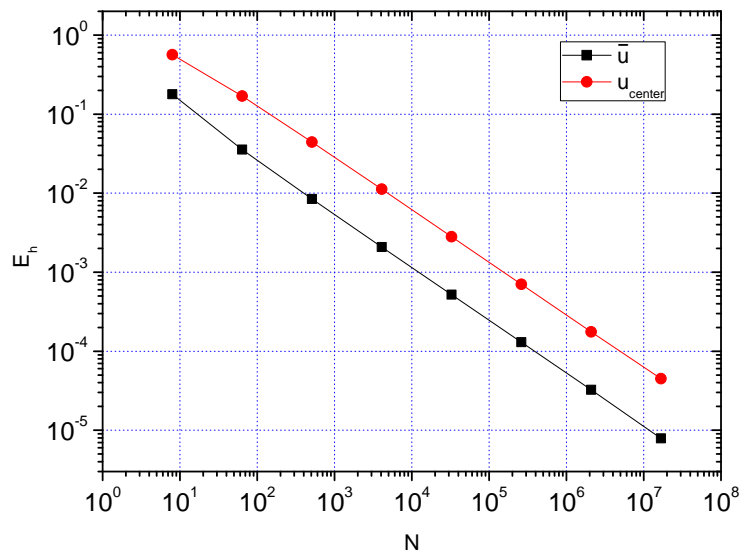


Figure 10: Poisson 3D, discretization error of the secondary variables

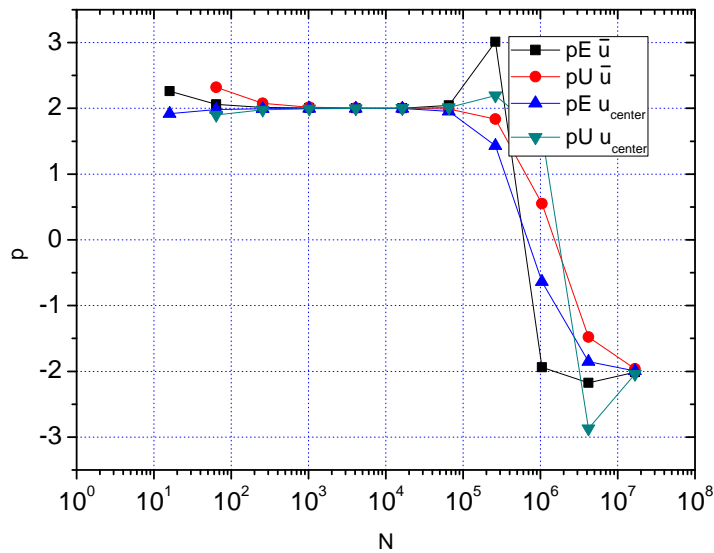


Figure 11: Poisson 2D, effective and apparent orders of the secondary variables

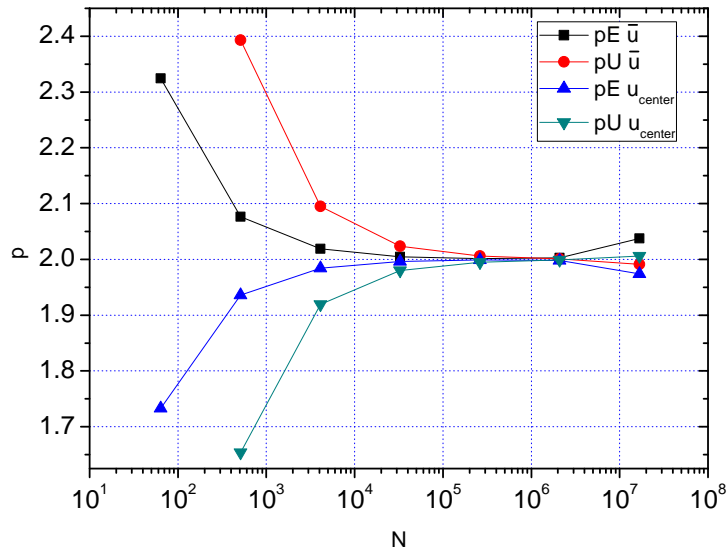


Figure 12: Poisson 3D, effective and apparent orders of the secondary variables

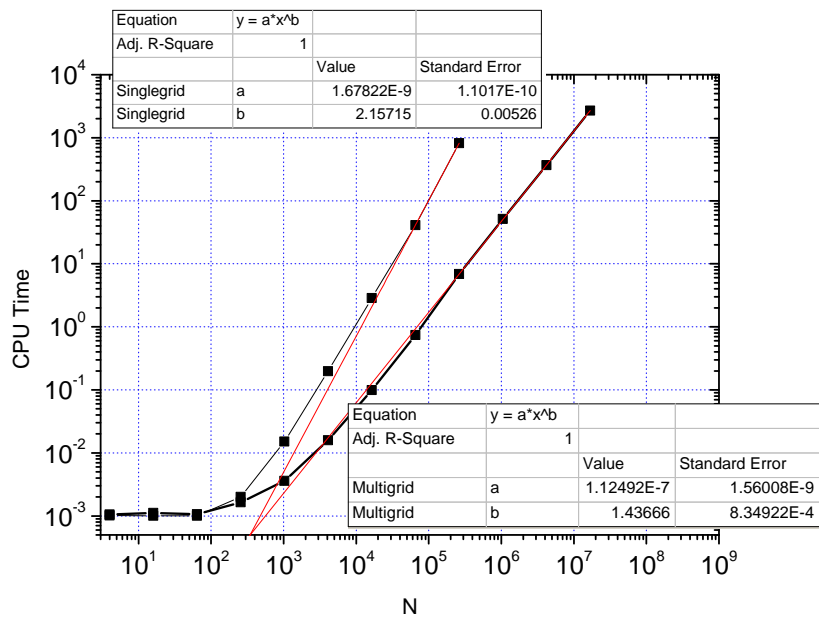


Figure 13: Poisson 2D, computational time with complexity coefficient

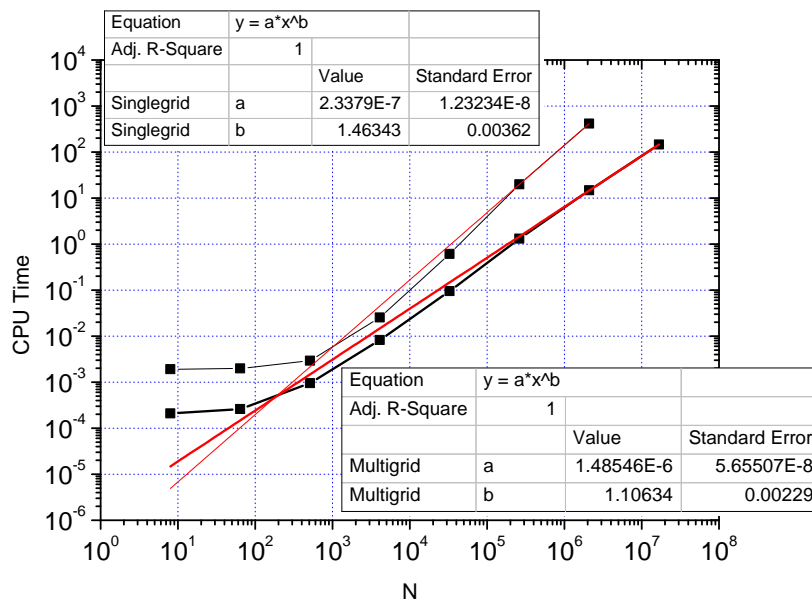


Figure 14: Poisson 3D, computational time with complexity coefficient